Chronic stress targets neurogenesis preferentially in the suprapyramidal blade of the rat dorsal dentate gyrus

Nuno D. Alves[1,2*], Patrícia Patrício[1,2*], Joana S. Correia[1,2], António Mateus-Pinheiro[1,2], Ana R. Machado-Santos[1,2], Eduardo Loureiro-Campos[1,2], Mónica Morais[1,2], João M. Bessa[1,2], Nuno Sousa[1,2], Luísa Pinto[1,2#]

[1]Life and Health Sciences Research Institute (ICVS), School of Medicine, University of Minho, Braga, Portugal

[2]ICVS/3B's - PT Government Associate Laboratory, Braga/Guimarães, Portugal

* These authors contributed equally to this work.

Correspondence to: luisapinto@med.uminho.pt

Nuno Dinis Lopes Oliveira Alves, MSc	Email: nunodloalves@med.uminho.pt
Patrícia Carvalho Patrício, PhD	Email: patriciapatricio@med.uminho.pt
Joana Sofia da Silva Correia, MSc	Email: joanacorreia@med.uminho.pt
António Maria Restolho Mateus-Pinheiro, PhD	Email: apinheiro@med.uminho.pt
Ana Rita Machado-Santos, MSc	Email: anarsantos@med.uminho.pt
Eduardo Manuel Loureiro-Campos, MSc	Email: eduardolc@med.uminho.pt
Mónica Susana Dias Morais, PhD	Email: monicamorais@med.uminho.pt
João Miguel Seiça Bessa Peixoto, MD PhD	Email: joaobessa@med.uminho.pt
Nuno Jorge Carvalho Sousa, MD PhD	Email: njcsousa@med.uminho.pt

Luísa Alexandra Meireles Pinto, PhD (corresponding author)
Life and Health Sciences Research Institute (ICVS), School of Medicine, University of Minho
ICVS/3B's, PT Government Associate Laboratory, Braga/Guimarães, Portugal
Campus de Gualtar
4710-057 Braga, Portugal
Tel: +351253604947
Email: luisapinto@med.uminho.pt

Abstract

The continuous generation of new neurons and glial cells in the adult hippocampal dentate gyrus (DG), represents an important form of adult neuroplasticity, involved in normal brain function and behavior but also associated with the etiopathogenesis and treatment of psychiatric disorders. Despite the large number of studies addressing cell genesis along the septotemporal axis, data on the anatomical gradients of cytogenesis along the DG transverse axis is scarce, especially after exposure to stress. As such, we characterized both basal proliferation and survival of adult-born neural cells along the transverse axis of the rat dorsal DG, and after stress exposure. In basal conditions, both proliferating cells and newborn neurons and glial cells were preferentially located at the subgranular zone and suprapyramidal blade. Exposure to chronic stress induced an overall decrease in the generation of adult-born neural cells and, more specifically, produced a regional-specific decrease in the survival of adult-born neurons at the suprapyramidal blade. No particular region-specific alterations were observed on surviving adult-born glial cells.

This work reveals, for the first time, a distinct survival profile of adult-born neural cells, neurons and glial cells, among the transverse axis of the DG, in both basal and stress conditions. Our results unveil that adult-born neurons are preferentially located in the suprapyramidal blade and suggest a regional-specific impact of chronic stress in this blade with potential repercussions for its functional significance.

Keywords

Dentate gyrus; Transverse axis; Cytogenesis; Proliferation; Survival; Chronic Stress;

Introduction

In the adult rat hippocampus, the generation of new neurons and glial cells occurs from neural stem cells (NSCs) located in the subgranular zone (SGZ) of the dentate gyrus (DG), between the granule cell layer (GCL) and the hilus (Ming and Song 2011; Patricio et al. 2013). The processes of neuro- or gliogenesis encompass several steps, from the proliferation of progenitor cells to the maturation of the newly generated cells and the establishment of appropriate synaptic contacts that culminate with their integration on the pre-existing network (Patricio et al. 2013). New hippocampal neurons start receiving synaptic inputs (Esposito et al. 2005; Overstreet Wadiche et al. 2005) and establish synapses with *Cornus Ammonis* 3 (CA3) pyramidal neurons during the first weeks after birth (Faulkner et al. 2008; Toni et al. 2008). Interestingly, immature adult-born neurons, namely at 4 weeks of age, display distinct properties from their mature counterparts. These include heightened synaptic plasticity (Gu et al. 2012) that may confer an advantage in the competition for synaptic connections (Tashiro et al. 2006; Toni et al. 2007) and allow these adult-born neurons to especially contribute to information processing during this period (Gu et al. 2012; Ming and Song 2011). After a maturation phase, around 4 to 8 weeks after birth, adult-born neurons present electrophysiological properties comparable to mature neurons (Aimone et al. 2010). Interestingly, these adult-born neurons have been proposed to participate in stress response (Snyder et al. 2011) and antidepressants' actions (Alves et al. 2017; Miller and Hen 2015), and in diverse cognitive tasks, including pattern separation (Aimone et al. 2011), contextual and spatial memory (Deng et al. 2010) and memory consolidation (Kitamura et al. 2009).

Astrocytes are also generated from NSCs in the adult hippocampal DG. However, the functional relevance of adult-born astrocytes and the regulation of their differentiation process remain largely undetermined (Rajkowska and Miguel-Hidalgo 2007). Interestingly, the existence of distinct subsets of progenitor cells committed to a glial lineage has been recently proposed (Encinas et al. 2011; Encinas et al. 2013). Resident and fully differentiated hippocampal mature astrocytes are known to play a crucial role in local neuronal activity and function, and to regulate the process of

adult neurogenesis through the release of growth and neurotrophic factors (Horner and Palmer 2003; Seri et al. 2001; Song et al. 2002; Ueki et al. 2003). Astrocytes are also involved in the neural circuit development (Clarke and Barres 2013) and required for neuronal energy supply (Iadecola and Nedergaard 2007; Schousboe and Waagepetersen 2006).

Importantly, before the integration in the circuitry and along the maturation process, adult-born cells undergo a critical period of selection, in which, by apoptosis, the number of newly-born cells significantly decreases within few days (Biebl et al. 2000; Kuhn et al. 2005). In fact, only a fraction of these cells survive and is able to integrate and establish functional connections.

In light of the functional segregation along the septotemporal axis of the hippocampus, suggesting an association between the dorsal pole to cognitive regulation and ventral to emotional behavior (Fanselow and Dong 2010; Tanti and Belzung 2013; Wu et al. 2015), it became plausible to expect that adult-born cells generated in the hippocampal DG may present different properties, depending on the location in which they integrate. Furthermore, the DG can be divided across a transverse axis, into the suprapyramidal blade, located between CA1 and CA3, and the infrapyramidal blade on the opposite side of the hilus (Wu et al. 2015). Previous studies have revealed a dissociation between these two blades, as they differ in their granule cell structure and physiology (Claiborne et al. 1990), excitability (Chawla et al. 2005; Ramirez-Amaya et al. 2005), response to stimulation (Scharfman et al. 2002) and gene expression pattern (Kanatsou et al. 2015). The heterogeneity along the DG transverse axis suggests that the two blades may differently contribute to hippocampal function. Most likely, the location in which adult-generated cells integrate and establish their contacts within the pre-existing DG network may determine their functional significance. Few studies have addressed the gradients of neurogenesis along the transverse axis of the DG under basal conditions, reporting increased neurogenesis in the suprapyramidal blade compared with the infrapyramidal (Ambrogini et al. 2000; Dranovsky et al. 2011; Jinno 2011; Kempermann et al. 2003; Ramirez-Amaya et al. 2006).

Chronic stress severely impacts the generation of adult-born cells in the DG, which have been recognized as relevant players in the development and recovery of behavioral deficits, namely cognitive and emotional, that underlie several neuropsychiatric disorders (Mateus-Pinheiro et al. 2013a; Mateus-Pinheiro et al. 2013b; Snyder et al. 2011). The functional anatomical dissociation along the hippocampus is also reflected in response to these and other stimuli (O'Leary and Cryan 2014; O'Leary et al. 2014; Pinto et al. 2015; Tanti and Belzung 2013). However, while, most studies focusing on the impact of chronic stress in hippocampal cytogenesis have considered the entire DG or discriminated between the dorsal and ventral poles, the structural segregation along its transverse axis has not been explored. Thus, herein we assessed the basal gradients of proliferation and cell survival across the transverse axis of the dorsal DG and after chronic stress exposure.

Materials and Methods

Animals

Experiments were conducted in adult male (2-months old) Wistar Han rats (Charles River Laboratories, L'Arbresle, France) housed and kept under standard laboratory conditions: 22 ± 1ºC, 55% relative humidity, 12 h light/dark cycle, food and water *ad libitum*. Rats were randomly divided into two experimental groups: a group of animals exposed to unpredictable chronic mild stress (uCMS) protocol and another not exposed to uCMS (CTRL), next described in detail. All procedures were conducted in accordance with EU Directive 2010/63/EU and the Portuguese National Authority for animal experimentation, *Direcção Geral de Alimentação e Veterinária*.

Unpredictable chronic mild stress (uCMS)

A previously described (Bessa et al. 2009; Mateus-Pinheiro et al. 2013b; Willner 2005) and validated uCMS protocol was applied for a 6-week period. This stress paradigm induces depressive-like behavior, anxiety-like phenotype and cognitive deficits in rats through random and

unpredictable exposure to a wide range of different mild stressors. The uCMS protocol included distinct stressors such as confinement to a restricted space for 1 h, placement in a tilted cage (30º) for 3 h, housing on damp bedding for 8 h, removal of sawdust for 3 h, overnight illumination, 15 h of food deprivation followed by exposure to inaccessible food for 1 h, water deprivation for 15 h followed by exposure to an empty bottle for 1 h, exposure to stroboscopic lights during 4 h, replacement of sawdust by cold water (4ºC) for 2 h, switch of cagemates for 2 h and reversed light/dark cycle for 48 h, every 7 days.

Four weeks before the initiation of the uCMS protocol, all animals received intraperitoneal injections of bromodeoxyuridine (BrdU, 50 mg/kg; Sigma Aldrich, St. Louis, MO, USA) during 7 consecutive days to label newly generated adult-born cells (**Fig. 2a**).

Behavioral analysis

At the end of the uCMS protocol, behavioral tests (n= 8 per group) were performed to evaluate cognitive traits related to hippocampal function. The Morris water maze (MWM) test was applied to evaluate working and spatial reference memory, as well as behavioral flexibility. In addition, the novel object recognition (NOR) test was performed to assess long-term and object location memory.

Morris water maze (MWM) test

The MWM paradigm was performed as previously described (Cerqueira et al. 2007). The water maze consisted in a black circular tank (diameter: 170 cm; depth: 50 cm), filled with water (23 ± 1ºC; 31 cm of depth) placed in a dimly lit room with extrinsic clues on the surrounding walls. The water tank was divided in four imaginary quadrants and a black escape platform (12 cm diameter; 30 cm high), invisible to rodents, was placed in the center of a quadrant. Trials were video-captured by a video-tracking system (Viewpoint, Champagne au Mont d'Or, France).

Working memory task

The working memory task was used to evaluate a cognitive domain that relies on the interplay between hippocampal and prefrontal cortex functions (Cerqueira et al. 2007; Kesner 2000). An escape platform was placed in one of the quadrants and there maintained during the four daily trials. The test was performed during four consecutive days, and in each day the platform was repositioned in a different quadrant. The goal of the task was to learn the position of the hidden platform and retain this information along the daily trials. For each trial, rats were placed in the water facing the wall in each of the quadrants (north, east, west or south). A trial was considered concluded when animals reached the platform, within the time limit of 120 seconds. The escape latency time was recorded for each trial. Performance in this task was also achieved by analyzing the area under the curve (AUC) (Youngblood et al. 1997) and the slopes of the linear regressions of the escape latency curves (as a index of the learning capacities) (Drouin et al. 2011).

Spatial reference memory task

Following the working memory task (days 1-4), spatial reference memory, a hippocampal-dependent function (Morris 1984) was assessed by maintaining the platform in the same quadrant during three consecutive days (days 4-6). Animals were tested in four daily trials, in accordance to the previously described procedure. Escape latency time on days 4-6 was recorded and analyzed. As before, performance in the reference memory task was also determined by the AUC and the learning slope.

Search strategies were defined as previously described (Garthe and Kempermann 2013; Mateus-Pinheiro et al. 2016; Ruediger et al. 2012). Quantitative analyses and strategy categorization was performed with data collected by the Viewpoint software, using an algorithm for systematized strategy attribution. This was based on the following parameters: (i) thigmotaxis (Tt): >70% of swam distance within the outer ring area (8 cm from the pool border); (ii) random swim (RS): >80% of swam distance within the inner circular area; balanced quadrant exploration (all quadrants

explored with a percentage of swam distance not >50% for none of the quadrants); non-circular trajectory; (iii) scanning (Sc): >80% of swam distance within the inner circular area; balanced quadrant exploration (all quadrants explored with a percentage of swam distance not >50% for none of the quadrants); non-circular trajectory; percentage of swam distance in the platform corridor area (funnel shaped area centered along the imaginary axis connecting the start position and platform position) ≤60%; (iv) chaining (Ch): >80% of swam distance within the inner circular area; balanced quadrant exploration (all quadrants explored with a percentage of swam distance not >50% for none of the quadrants); percentage of swam distance in the platform corridor area ≤60%; circular trajectory (v) directed search (DS): >80% of swam distance within the inner circular area; percentage of swam distance in the platform corridor area >60% with shifts in the trajectory direction (vi) focal search (FS): percentage of swam distance in the perimeter of the escape platform (30 cm perimeter) > 50%; (vii) direct swim (DSw): >80% of swam distance within the inner circular area; percentage of swam distance in the platform corridor area >90% with no shifts in the trajectory direction ("direct trajectory").

For strategy blocks analysis, two blocks of strategies were defined: Block1, comprising the "non-hippocampal-dependent strategies" (Tt, RS and Sc) and Block2, comprising the "hippocampal-dependent strategies" (DS, FS and DSw). Strategy blocks were defined as a sequence of at least three trials with the strategies from the same category. For block lengths, a maximum of two-trial interruptions were tolerated but not counted: e.g. in the following strategies sequence "DS-DS-FS-DS-Sc-DS-FS-FS", the block length for Block2 was scored 8, despite the presence of one trial in which the attributed strategy belongs to Block1 (Sc). Independent analysis was performed for CTRL and uCMS animals.

Behavioral flexibility task

On day 7, animals were tested in a reverse learning task (a prefrontal cortex-dependent paradigm (de Bruin et al. 1994)) by positioning the platform into a new (opposite) quadrant. Rats were tested

in a four-trial paradigm, as described above, and the time-spent swimming in each quadrant was recorded. The percentage of time spent in the new quadrant containing the platform was used as a measure of reversal performance.

Novel object recognition (NOR)

Long-term memory and object location memory was assessed using the NOR test. Rats were first familiarized to the testing arena consisting of a black acrylic box (50 x 50 x 150 cm) with an open-field space, for 8 minutes, with no objects presentation. On the following day, animals were allowed to freely explore two identical objects for 10 minutes. One hour later, animals were tested in an object location task for 3 minutes, where one of the objects was relocated to the opposite corner of the testing arena. Twenty-four hours after the first 10 minutes trial, animals returned to the arena for 3 minutes, with one of the objects replaced by a novel one (long-term memory task). The familiar and novel objects differed on size, shape, texture and color. The NOR arena was cleaned with 10% ethanol between trials to avoid odor cues. All sessions were videotaped and the time spent exploring both objects was determined manually. Analysis was conducted blindly. The percentage of time spent exploring the novel/relocated object was used as a measure of long-term/object location memory performance, respectively.

Immunostaining procedures

Animals (n=3/4 per group) were deeply anaesthetized with sodium pentobarbital (20%; Eutasil®, Sanofi, Gentilly, France) and transcardially perfused with phosphate buffered saline (PBS) followed by cold 4% paraformaldehyde (PFA). Brains were removed, post-fixed in 4% PFA, cryoprotected in 30% sucrose overnight, and then embedded in Optimal Cutting Temperature compound (OCT, ThermoScientific, Waltham, MA, USA), snap-frozen and stored at -20ºC. Coronal sections (20 µm) containing the dorsal pole of the hippocampal dentate gyrus (DG) were further stained to assess cell

proliferation rates and the survival of adult-born neurons and astroglial cells. Sections were double-stained with BrdU (#6326; 1:100; Abcam, Cambridge, UK) and NeuN (#AB377, 1:100; Millipore, Temecula, CA, USA) to label mature adult-born neurons or GFAP (#20334, 1:200; Dako, Glostrup, Denmark) to label adult-born astrocytes. Cell proliferation rates were determined by the quantification of the total number of Ki-67^{+} (#AB9260, 1:300; Millipore) cells per area. Cell nuclei were stained with 4',6-diamidino-2-phenylindole (DAPI, 1:200; Sigma Aldrich). In addition to the total number of cells per DG, this region was also distinguished along its transverse axis, by determining the density of positive cells individually in the suprapyramidal and infrapyramidal blades. The density of positive cells was also determined in two other DG subregions: the granule cell layer (GCL) and the subgranular zone (SGZ), defined as the three deepest rows of granule cells, bordering the hilus (Miller et al. 2013; Silva et al. 2006).

The density of each cell population in the DG was determined by the ratio of the total number of cells and the respective area. Analysis and cell counting were performed using a confocal microscope (Olympus FluoViewTM FV1000, Hamburg, Germany) and each area was determined using an optical microscope (Olympus BX51). Observers were blind to the experimental condition of each subject. Cell densities are reported as number of cells *per* mm^2. To determine the contribution of specific DG areas for structural and functional alterations, we calculated the proportion of immunopositive-cells and compared between the DG subregions including supra- *vs* infrapyramidal blades, GCL *vs* SGZ, suprapyramidal GCL *vs* suprapyramidal SGZ, infrapyramidal GCL *vs* infrapyramidal SGZ, suprapyramidal GCL *vs* infrapyramidal GCL and suprapyramidal SGZ *vs* infrapyramidal SGZ. Relative proportions were determined by taking into consideration the densities of immunopositive-cells by the corresponding area as follows: *density of immunopositive cells in subregion 1 (number of positive-cells / corresponding DG area) / (density of immunopositive cells in the subregion 1 + density of immunopositive cells in subregion 2).* The impact of chronic stress exposure was calculated as fold difference between the density of cells in

animals exposed to uCMS and the median value of cell density of non-stressed animals in each subregion.

RT-PCR measurements

mRNA expression levels of the brain-derived neurotrophic factor (*Bdnf*) gene were measured by qRT-PCR. Total RNA was isolated from macrodissected DG (n=4 per group) using the Direct-zol™ RNA MiniPrep (Zymo Research, Irvine, CA, USA) according to the manufacturer's instructions. Obtained RNA (500 ng) was reverse transcribed using qScript cDNA SuperMix (Quanta Biosciences, Gaithersburg, MA, USA). Beta-2-Microglobulin (*B2m*) was used as internal standard for normalization of the target gene's expression. Oligonucleotide primers for *Bdnf* (sense: GGACCCTGAGTTCCACCA, antisense: CGTGCTCAAAAGTGTCAGCC) and *B2m* (sense: GTGCTTGCCATTCAGAAAACTCC, antisense: AGGTGGGTGGAACTGAGACA) were designed using Primer-BLAST software (NCBI). Real-time reactions were performed in a 7500 Fast-Real Time PCR System (Applied Biosystems, Foster City, CA, USA) using 5x HOT FIREPol EvaGreen qPCR Mix Plus (ROX) (Solis Biodyne, Tartu, Estonia). The relative expression was calculated using the ΔΔCt method. Results are presented as relative expression to the standard gene.

Corticosterone levels measurement

Serum corticosterone levels were measured in all animals (n=8 per group) using a commercially available ELISA kit (Enzo Life Sciences, Farmingdale, NY, USA), according to the manufacturer's instructions. Sampling (tail venipuncture) was performed between 8 and 9 a.m., after the last exposure to stress. Results are expressed as ng of corticosterone *per* ml of serum.

Statistical analysis

Statistical analysis was performed using GraphPad Prism 6.0 (GraphPad Software, Inc., La Jolla, CA, USA). Animals were randomly assigned to the experimental groups. All presented data

satisfied normal distribution in Kolmogorov–Smirnov testing. After confirmation of homogeneity of group variances, data was subjected to the appropriate statistical tests. Student's *t*-test was used for statistical comparisons between experimental groups when appropriate. Analysis of variance repeated measures was used to analyze cognitive learning tasks in the MWM. Descriptive statistical results are presented as mean ± standard error of the mean (SEM). Differences between groups were determined by Bonferroni's *post-hoc* multiple comparison test and statistical significance was set at $P < 0.05$.

Results

Proliferating and newborn cells are not evenly distributed along the dorsal hippocampal DG

Literature has pinpointed the relevance of dividing the DG structure into distinct subregions (Amaral et al. 2007; Tannenholz et al. 2014; Wu et al. 2015). In this study, we have focused on the dorsal hippocampal DG, a brain region where new cells are born throughout adult life, to analyze the distribution of proliferating and newly born cells along its transverse axis, in basal conditions (**Fig. 1a**). Expectedly, the majority of Ki-67^{+} proliferating cells was located at the SGZ in a proportion of ≈19:1 to the GCL (Jabes et al. 2010; Nieto-Estevez et al. 2016) (P = 0.0001; **Figure 1b**). This was also observed when considering only the suprapyramidal or the infrapyramidal portions (supra: P < 0.0001; infra: P = 0.005; **Figure 1b**). Moreover, our analysis along the transverse axis of the total dorsal DG revealed a higher proportion of Ki-67^{+} cells in the suprapyramidal blade (≈3:2) (P = 0.0038; **Fig. 1c**). However, considering the subregions SGZ and GCL separately, we did not observe significant differences between the infra- and the suprapyramidal blades (**Fig. 1c**).

To assess the distribution of surviving adult-born cells in the DG, animals were injected with the thymidine analog and exogenous S-phase marker, BrdU, 10 weeks prior to sacrifice (**Fig. 1a**). Cell fate was determined by co-localization of BrdU^{+} cells with the marker of neuronal maturation, NeuN or with the astroglial cell marker, GFAP (**Fig. 1d-g, Table 1 and 2)**. Interestingly, most adult-born neurons were located in the SGZ compared to the GCL (≈9:1; P = 0.0007; **Fig. 1d**). The same tendency was observed for adult-born astroglial cells (**Fig. 1f**). Additionally, newborn neurons were mostly found at the suprapyramidal blade, although only reaching significant differences in the GCL (P = 0.0012; **Fig. 1e**). No significant differences were found, in the distribution of astroglial newborn cells, between the infra- and suprapyramidal blades (**Fig. 1g**).

Chronic stress induces cognitive deficits in hippocampal-dependent tasks

Chronic stress is one of the most widely studied stimuli known to produce behavioral and neuroplastic deficits in several brain regions. As previously described (Smith et al. 1995; Tsankova et al. 2006) chronically stressed animals presented increased serum corticosterone levels (P = 0.0199, **Fig. 2b**) and decreased *Bdnf* gene expression levels in the hippocampal DG when compared to CTRL animals (P = 0.0490, **Fig. 2c**). The impact of the uCMS protocol exposure was also evaluated on hippocampal-dependent functions, specifically in cognitive tasks (**Fig. 2d-j**). Chronic stress exposure impaired long-term and object location memory in the NOR test, as denoted by a decreased exploration of the novel ($P < 0.0001$, **Fig. 2d)** and of the relocated object (P = 0.0465, **Fig. 2e**), respectively. Performance in working and reference memory tasks was evaluated in the MWM test. Despite no observed impact of uCMS in working memory (**Supp. Fig. 1**), stressed animals presented significant impairments in the reference memory task, particularly evident in the second day of the test (day2: P = 0.0365, **Fig. 2f**). These deficits were further corroborated by significant alterations in the AUC latency (P = 0.0021, **Fig. 2f**). Importantly, uCMS-exposed animals presented a delayed transition from non-hippocampal-dependent strategies (Block 1) to hippocampal-dependent strategies (Block 2) (CTRL: P = 0.0096; uCMS: P = 0.0118, **Fig. 2h-j**) in the reference memory task of the MWM. Animals subjected to uCMS also presented deficits in the behavioral flexibility task (P = 0.0001, **Fig. 2g**).

uCMS evenly decreases proliferation in the dorsal DG subregions

We next assessed the impact of chronic stress exposure in the cytogenic process in dorsal DG subregions (**Fig. 3a-c and Supp. Fig. 2-4)**. As previously described (Bessa et al. 2009; Nollet et al. 2012), uCMS decreased the total number of proliferating Ki-67$^+$ cells in the DG (P = 0.0261, **Fig. 3a**), Considering the DG transverse axis, uCMS reduced the number of Ki-67$^+$ cells in both supra- and infrapyramidal blades of the total DG (supra DG: P = 0.0495; infra DG: P = 0.0439, **Figure 3a**). In addition, chronic stress significantly decreased the number of proliferating cells in both the SGZ and GCL subdivisions (SGZ: P = 0.0353; GCL: P = 0.0387, **Fig. 3a and Supp. Fig. 2**).

Chronic stress impacts the survival of adult-born neurons particularly in the suprapyramidal blade of the DG

To assess the impact of the 6-week uCMS protocol in the survival of adult-born neurons in the DG, animals were injected with BrdU, 4 weeks prior to stress exposure, to label newborn cells (**Fig. 2a**). The number of double-labeled $BrdU^+NeuN^+$ was assessed in the dorsal DG subregions (**Fig. 3b and Supp. Fig.3**). As expected, uCMS decreased the overall survival of adult-born neurons in the hippocampal DG (P = 0.0308, **Fig. 3b**). Interestingly, chronic stress specifically affected the survival of adult-born neurons in the suprapyramidal but not in the DG infrapyramidal blade (supra DG: P = 0.0019, infra DG: P = 0.4918, **Fig. 3b**). As such, while CTRL animals present a preferential distribution of $BrdU^+NeuN^+$ cells in the suprapyramidal blade (≈7:3), animals exposed to uCMS, present a preferential survival of cells in the infrapyramidal blade (≈1:3, P = 0.0257). Additionally, we could not disclose statistically significant changes induced by chronic stress in the SGZ and GCL regions (SGZ: P = 0.1507; GCL: P = 0.4874, **Fig. 3b**).

uCMS decreases the survival of adult-born astroglial cells in the DG in a non-subregion-specific manner

Finally, we assessed the impact of uCMS in the survival of adult-born astroglial cells by determining the density of $BrdU^+$ cells that co-labeled with the glial marker GFAP in the previously defined DG subregions (**Fig. 3c** and **Supp. Fig. 4**). Whole dorsal DG analysis revealed a significant decrease in the number of $BrdU^+GFAP^+$ newborn astroglial cells after uCMS exposure (P = 0.0461, **Fig. 3c** and **Table 1** and **2**). However, and contrarily to its effect in the survival of newly-born neurons, exposure to uCMS did not significantly impact in the survival of adult-born astroglial cells in any of the DG subregions compared to CTRL animals (P > 0.1, **Figure 3c**).

An overview of the distribution of different cell populations throughout the dorsal DG subregions, as well the uCMS-induced alterations are summarized in **Figure 3d-g** and **Table 3**.

Discussion

In the adult rat hippocampal DG, a large number of new neurons and glial cells are continuously generated, however within 4-weeks after birth, only a fraction (20-40%) survives and is able to functionally integrate the pre-existing networks (Cameron and McKay 2001; Dayer et al. 2003). Adult-born neurons, in particular those generated in the dorsal DG, have been implicated in diverse cognitive functions, including memory formation (Shors et al. 2001) and pattern separation (Aimone et al. 2010; Kheirbek et al. 2012). Less well understood is the role of adult-born astrocytes. Since the hippocampus is viewed as a functionally heterogeneous structure with a well-demarked longitudinal axis, studies have lately focused on the relevance of the generation of new cells in the dorsal and ventral hippocampus, two anatomically and physiologically distinct subregions (Fanselow and Dong 2010). However, few pieces of evidence have addressed this topic along the transverse axis of the DG. In the present work, we have focused on the dorsal part of the hippocampal DG, to assess the gradients of proliferation and cell survival across its transverse axis, in basal conditions and after chronic stress exposure.

In basal conditions, and similarly to previous studies (Ambrogini et al. 2000; Dranovsky et al. 2011; Jinno 2011; Kempermann et al. 2003; Ramirez-Amaya et al. 2006), we observed a slightly increased survival of adult-born neurons and astroglial cells in the DG suprapyramidal blade. This regional preference could result from distinct microenvironments in both subregions, which may favor the survival of adult-born cells in the suprapyramidal portion *versus* the infrapyramidal blade. Interestingly, cells in the suprapyramidal blade show greater experience-related neuronal activity in the water maze (Snyder et al. 2009b) or following exploration of a novel environment (Chawla et al. 2005; Pace et al. 2005; Satvat et al. 2012; Snyder et al. 2009b; VanElzakker et al. 2008). Contrastingly, others have observed increased cell proliferation (Olariu et al. 2007; Snyder et al. 2009b) and survival (Choi et al. 2007) in the infrapyramidal blade. In those studies, BrdU was used to assess fast-proliferating cells instead of Ki-67 (Olariu et al. 2007; Snyder et al. 2009b) or the

BrdU injection paradigm for survival was different from the one performed here (Choi et al. 2007), possibly accounting for the distinct results.

Granule neurons from the suprapyramidal blade present increased dendritic length, more dendritic segments, wider dendritic spreads (Claiborne et al. 1990) and increased spine density (Desmond and Levy 1985) compared to the infrapyramidal blade [reviewed by (Rahimi and Claiborne 2007)]. Taken together, this indicates that granule neurons in the suprapyramidal portion receive more synaptic afferent contacts. The morphological and physiological differences between the supra- and infrapyramidal blades, and the regional preferences described herein, suggest that they contribute differently to specific behaviors. Moreover, these specificities may have major implications, namely for cell-specific targeting in optogenetic manipulations and electrophysiology studies.

In line with previous studies showing that stress impacts on hippocampal proliferation and neuronal and glial cells survival (Bessa et al. 2009; Egeland et al. 2015; Mateus-Pinheiro et al. 2013a; Mateus-Pinheiro et al. 2013b), we observed that chronic stress impacted the ongoing proliferation of neural progenitor cells and the survival of both 4-weeks old neurons and glial cells.

There are critical periods for the survival of adult-born neurons along the neurogenic process; early, when cells become post-mitotic (late phase of DCX expression), and later, following the integration when newborn neurons present increased synaptic plasticity (Ge et al. 2007). Thus, it is plausible that deleterious stimuli, including chronic stress, during these specific stages of the neurogenic process have important behavioral repercussions. Specifically at 4 weeks of age, when the projections of the DG to the CA3 area become stable, neurons are particularly important for retrieval of hippocampal memory (Gu et al. 2012; Mateus-Pinheiro et al. 2013b). Whether cells at this developmental stage are particularly sensitive to the effects of chronic stress remains to be determined. Our results highlight the importance of tackling different stages of the neurogenic period to assess their specific contribution for brain physiology and behavior.

When discriminating the effects of uCMS along the transverse axis of the DG, we found that uCMS decreased the number of proliferating cells to a similar extent in all considered regions. Noticeably,

chronic stress exposure impacted specifically in adult-born neurons survival at the suprapyramidal blade. On the other hand, uCMS-exposure did not specifically impact on the survival of glial cells in this subregion, which may be attributed to the small number of newborn astrocytes and the relatively small sample size. The preferential impact of chronic stress on the survival of adult-born neurons in the suprapyramidal blades is in line with previous findings showing a specific increased activation (Fos expression) of the granule neurons in the suprapyramidal blade after restraint stress (Chowdhury et al. 2000; Fevurly and Spencer 2004); interestingly, activation of the suprapyramidal blade was reduced in adrenalectomized rats (Fevurly and Spencer 2004). In contrast, however, a previous work in mice reported that chronic stress decreased the number of immature DCX^+ neurons specifically in the infrapyramidal blade, but not of 3-weeks old $BrdU^+$ cells (Kanatsou et al. 2015). Of note, the magnitude and maturation dynamics of hippocampal cytogenesis are different between rats and mice, probably accounting for these apparently divergent findings (Snyder et al. 2009a). The specific vulnerability of adult-born neurons in the suprapyramidal blade to the deleterious effects of chronic stress could result from several factors. A distinct expression profile of glucocorticoid (GR), mineralocorticoid (MR) receptors, neurotransmitters receptors, and neurotrophic factors and their receptors along the transverse axis (Toyoda et al. 2014) may at least partly explain this regional-specific susceptibility to chronic stress. Although originated from identical progenitor cells, possible differences in adult-born neurons at infra- and suprapyramidal layers may arise from their specific network circuitry. Indeed, the suprapyramidal blade receives twice as many projections from subcortical regions as the infrapyramidal blade; these subcortical regions include the septal nucleus, locus coeruleus, raphe nucleus, and the supramammilary nucleus (Schmidt et al. 2012; Wyss et al. 1979). In particular, the supramammilary nucleus is an important pacemaker of hippocampal theta rhythms (Kocsis and Vertes 1997; Vinogradova 1995). These are selectively present during exploratory behavior and REM sleep, and assumed to serve a critical role in memory and navigation (Buzsaki and Moser 2013; O'Keefe and Nadel), two of the behavioral domains affected by this chronic stress exposure paradigm.

Altogether, in the present study, we found that the generation of new cells in the hippocampus is not uniform along the transverse axis of the septal DG. Moreover, chronic stress was shown to decrease the survival of adult-born neurons, but not glial cells, specifically in the suprapyramidal blade, which may relate to the cognitive deficits observed in these animals.

Similarly to the well described functional differences between the dorsal and the ventral DG (Kheirbek et al. 2013; Kheirbek and Hen 2011; Wu et al. 2015), as well as the proposed distinct contributions levels of neurogenesis along this septotemporal axis (both in basal conditions (Snyder et al. 2009b) or after chronic stress (Brummelte and Galea 2010; Jayatissa et al. 2006; Tanti et al. 2012)), we suggest that, in light of the present work, upcoming studies targeting the processes of adult hippocampal neurogenesis and astrogliogenesis should consider the dissociation of the DG into their supra- and infrapyramidal blades.

Funding

NDA, PP, AMP, ARMS, MM and LP received fellowships from the Portuguese Foundation for Science and Technology (FCT). This work was funded by FCT (IF/01079/2014).

This article has been developed under the scope of the project NORTE-01-0145-FEDER-000013, supported by the Northern Portugal Regional Operational Programme (NORTE 2020), under the Portugal 2020 Partnership Agreement, through the European Regional Development Fund (FEDER).

This work has been funded by FEDER funds, through the Competitiveness Factors Operational Programme (COMPETE), and by National funds, through the Foundation for Science and Technology (FCT), under the scope of the project POCI-01-0145-FEDER-007038.

Conflict of Interest

The authors declare no conflicts of interest.

References

Aimone JB, Deng W, Gage FH (2010) Adult neurogenesis: integrating theories and separating functions Trends Cogn Sci 14:325-337 doi:S1364-6613(10)00088-4 [pii]
10.1016/j.tics.2010.04.003

Aimone JB, Deng W, Gage FH (2011) Resolving new memories: a critical look at the dentate gyrus, adult neurogenesis, and pattern separation Neuron 70:589-596 doi:10.1016/j.neuron.2011.05.010

Alves ND et al. (2017) Adult hippocampal neuroplasticity triggers susceptibility to recurrent depression Transl Psychiatry 7:e1058 doi:10.1038/tp.2017.29

Amaral DG, Scharfman HE, Lavenex P (2007) The dentate gyrus: fundamental neuroanatomical organization (dentate gyrus for dummies) Prog Brain Res 163:3-22 doi:10.1016/S0079-6123(07)63001-5

Ambrogini P et al. (2000) Spatial learning affects immature granule cell survival in adult rat dentate gyrus Neurosci Lett 286:21-24

Bessa JM et al. (2009) The mood-improving actions of antidepressants do not depend on neurogenesis but are associated with neuronal remodeling Molecular psychiatry 14:764-773, 739 doi:10.1038/mp.2008.119

Biebl M, Cooper CM, Winkler J, Kuhn HG (2000) Analysis of neurogenesis and programmed cell death reveals a self-renewing capacity in the adult rat brain Neurosci Lett 291:17-20

Brummelte S, Galea LA (2010) Chronic high corticosterone reduces neurogenesis in the dentate gyrus of adult male and female rats Neuroscience 168:680-690 doi:10.1016/j.neuroscience.2010.04.023

Buzsaki G, Moser EI (2013) Memory, navigation and theta rhythm in the hippocampal-entorhinal system Nat Neurosci 16:130-138 doi:10.1038/nn.3304

Cameron HA, McKay RD (2001) Adult neurogenesis produces a large pool of new granule cells in the dentate gyrus J Comp Neurol 435:406-417

Cerqueira JJ, Mailliet F, Almeida OF, Jay TM, Sousa N (2007) The prefrontal cortex as a key target of the maladaptive response to stress J Neurosci 27:2781-2787 doi:27/11/2781 [pii] 10.1523/JNEUROSCI.4372-06.2007

Chawla MK et al. (2005) Sparse, environmentally selective expression of Arc RNA in the upper blade of the rodent fascia dentata by brief spatial experience Hippocampus 15:579-586 doi:10.1002/hipo.20091

Choi YS, Cho KO, Kim SY (2007) Asymmetry in enhanced neurogenesis in the rostral dentate gyrus following kainic acid-induced status epilepticus in adult rats Arch Pharm Res 30:646-652

Chowdhury GM, Fujioka T, Nakamura S (2000) Induction and adaptation of Fos expression in the rat brain by two types of acute restraint stress Brain Res Bull 52:171-182

Claiborne BJ, Amaral DG, Cowan WM (1990) Quantitative, three-dimensional analysis of granule cell dendrites in the rat dentate gyrus J Comp Neurol 302:206-219 doi:10.1002/cne.903020203

Clarke LE, Barres BA (2013) Emerging roles of astrocytes in neural circuit development Nat Rev Neurosci 14:311-321 doi:10.1038/nrn3484

Dayer AG, Ford AA, Cleaver KM, Yassaee M, Cameron HA (2003) Short-term and long-term survival of new neurons in the rat dentate gyrus J Comp Neurol 460:563-572 doi:10.1002/cne.10675

de Bruin JP, Sanchez-Santed F, Heinsbroek RP, Donker A, Postmes P (1994) A behavioural analysis of rats with damage to the medial prefrontal cortex using the Morris water maze: evidence for behavioural flexibility, but not for impaired spatial navigation Brain Res 652:323-333

Deng W, Aimone JB, Gage FH (2010) New neurons and new memories: how does adult hippocampal neurogenesis affect learning and memory? Nat Rev Neurosci 11:339-350 doi:10.1038/nrn2822

Desmond NL, Levy WB (1985) Granule cell dendritic spine density in the rat hippocampus varies with spine shape and location Neurosci Lett 54:219-224

Dranovsky A et al. (2011) Experience dictates stem cell fate in the adult hippocampus Neuron 70:908-923 doi:10.1016/j.neuron.2011.05.022

Drouin A et al. (2011) Catechin treatment improves cerebrovascular flow-mediated dilation and learning abilities in atherosclerotic mice Am J Physiol Heart Circ Physiol 300:H1032-1043 doi:10.1152/ajpheart.00410.2010

Egeland M, Zunszain PA, Pariante CM (2015) Molecular mechanisms in the regulation of adult neurogenesis during stress Nat Rev Neurosci 16:189-200 doi:10.1038/nrn3855

Encinas JM et al. (2011) Division-coupled astrocytic differentiation and age-related depletion of neural stem cells in the adult hippocampus Cell Stem Cell 8:566-579 doi:10.1016/j.stem.2011.03.010

Encinas JM, Sierra A, Valcarcel-Martin R, Martin-Suarez S (2013) A developmental perspective on adult hippocampal neurogenesis Int J Dev Neurosci 31:640-645 doi:10.1016/j.ijdevneu.2013.04.001

Esposito MS, Piatti VC, Laplagne DA, Morgenstern NA, Ferrari CC, Pitossi FJ, Schinder AF (2005) Neuronal differentiation in the adult hippocampus recapitulates embryonic development J Neurosci 25:10074-10086 doi:10.1523/JNEUROSCI.3114-05.2005

Fanselow MS, Dong HW (2010) Are the dorsal and ventral hippocampus functionally distinct structures? Neuron 65:7-19 doi:10.1016/j.neuron.2009.11.031

Faulkner RL et al. (2008) Development of hippocampal mossy fiber synaptic outputs by new neurons in the adult brain Proc Natl Acad Sci U S A 105:14157-14162 doi:10.1073/pnas.0806658105

Fevurly RD, Spencer RL (2004) Fos expression is selectively and differentially regulated by endogenous glucocorticoids in the paraventricular nucleus of the hypothalamus and the dentate gyrus J Neuroendocrinol 16:970-979 doi:10.1111/j.1365-2826.2004.01257.x

Garthe A, Kempermann G (2013) An old test for new neurons: refining the Morris water maze to study the functional relevance of adult hippocampal neurogenesis Front Neurosci 7:63 doi:10.3389/fnins.2013.00063

Ge S, Yang CH, Hsu KS, Ming GL, Song H (2007) A critical period for enhanced synaptic plasticity in newly generated neurons of the adult brain Neuron 54:559-566 doi:10.1016/j.neuron.2007.05.002

Gu Y, Arruda-Carvalho M, Wang J, Janoschka SR, Josselyn SA, Frankland PW, Ge S (2012) Optical controlling reveals time-dependent roles for adult-born dentate granule cells Nat Neurosci 15:1700-1706 doi:10.1038/nn.3260

Horner PJ, Palmer TD (2003) New roles for astrocytes: the nightlife of an 'astrocyte'. La vida loca! Trends Neurosci 26:597-603 doi:10.1016/j.tins.2003.09.010

Iadecola C, Nedergaard M (2007) Glial regulation of the cerebral microvasculature Nat Neurosci 10:1369-1376 doi:10.1038/nn2003

Jabes A, Lavenex PB, Amaral DG, Lavenex P (2010) Quantitative analysis of postnatal neurogenesis and neuron number in the macaque monkey dentate gyrus Eur J Neurosci 31:273-285 doi:10.1111/j.1460-9568.2009.07061.x

Jayatissa MN, Bisgaard C, Tingstrom A, Papp M, Wiborg O (2006) Hippocampal cytogenesis correlates to escitalopram-mediated recovery in a chronic mild stress rat model of depression Neuropsychopharmacology 31:2395-2404 doi:1301041 [pii]
10.1038/sj.npp.1301041

Jinno S (2011) Topographic differences in adult neurogenesis in the mouse hippocampus: a stereology-based study using endogenous markers Hippocampus 21:467-480 doi:10.1002/hipo.20762

Kanatsou S et al. (2015) Overexpression of Mineralocorticoid Receptors Partially Prevents Chronic Stress-Induced Reductions in Hippocampal Memory and Structural Plasticity PLoS One 10:e0142012 doi:10.1371/journal.pone.0142012

Kempermann G, Gast D, Kronenberg G, Yamaguchi M, Gage FH (2003) Early determination and long-term persistence of adult-generated new neurons in the hippocampus of mice Development 130:391-399

Kesner RP (2000) Behavioral analysis of the contribution of the hippocampus and parietal cortex to the processing of information: interactions and dissociations Hippocampus 10:483-490 doi:10.1002/1098-1063(2000)10:4<483::AID-HIPO15>3.0.CO;2-Z

Kheirbek MA et al. (2013) Differential control of learning and anxiety along the dorsoventral axis of the dentate gyrus Neuron 77:955-968 doi:10.1016/j.neuron.2012.12.038

Kheirbek MA, Hen R (2011) Dorsal vs ventral hippocampal neurogenesis: implications for cognition and mood Neuropsychopharmacology 36:373-374 doi:10.1038/npp.2010.148

Kheirbek MA, Klemenhagen KC, Sahay A, Hen R (2012) Neurogenesis and generalization: a new approach to stratify and treat anxiety disorders Nat Neurosci 15:1613-1620 doi:10.1038/nn.3262

Kitamura T et al. (2009) Adult neurogenesis modulates the hippocampus-dependent period of associative fear memory Cell 139:814-827 doi:10.1016/j.cell.2009.10.020

Kocsis B, Vertes RP (1997) Phase relations of rhythmic neuronal firing in the supramammillary nucleus and mammillary body to the hippocampal theta activity in urethane anesthetized rats Hippocampus 7:204-214 doi:10.1002/(SICI)1098-1063(1997)7:2<204::AID-HIPO7>3.0.CO;2-M

Kuhn HG, Biebl M, Wilhelm D, Li M, Friedlander RM, Winkler J (2005) Increased generation of granule cells in adult Bcl-2-overexpressing mice: a role for cell death during continued hippocampal neurogenesis Eur J Neurosci 22:1907-1915 doi:10.1111/j.1460-9568.2005.04377.x

Mateus-Pinheiro A et al. (2016) AP2gamma controls adult hippocampal neurogenesis and modulates cognitive, but not anxiety or depressive-like behavior Molecular psychiatry doi:10.1038/mp.2016.169

Mateus-Pinheiro A, Patricio P, Bessa JM, Sousa N, Pinto L (2013a) Cell genesis and dendritic plasticity: a neuroplastic pas de deux in the onset and remission from depression Mol Psychiatry 18:748-750 doi:10.1038/mp.2013.56

Mateus-Pinheiro A et al. (2013b) Sustained remission from depressive-like behavior depends on hippocampal neurogenesis Transl Psychiatry 3:e210 doi:10.1038/tp.2012.141

Miller BR, Hen R (2015) The current state of the neurogenic theory of depression and anxiety Curr Opin Neurobiol 30:51-58 doi:10.1016/j.conb.2014.08.012

Miller JA et al. (2013) Conserved molecular signatures of neurogenesis in the hippocampal subgranular zone of rodents and primates Development 140:4633-4644 doi:10.1242/dev.097212

Ming GL, Song H (2011) Adult neurogenesis in the mammalian brain: significant answers and significant questions Neuron 70:687-702 doi:S0896-6273(11)00348-5 [pii]
10.1016/j.neuron.2011.05.001

Morris R (1984) Developments of a water-maze procedure for studying spatial learning in the rat J Neurosci Methods 11:47-60

Nieto-Estevez V, Oueslati-Morales CO, Li L, Pickel J, Morales AV, Vicario-Abejon C (2016) Brain Insulin-Like Growth Factor-I Directs the Transition from Stem Cells to Mature Neurons During Postnatal/Adult Hippocampal Neurogenesis Stem Cells 34:2194-2209 doi:10.1002/stem.2397

Nollet M, Gaillard P, Tanti A, Girault V, Belzung C, Leman S (2012) Neurogenesis-independent antidepressant-like effects on behavior and stress axis response of a dual orexin receptor antagonist in a rodent model of depression Neuropsychopharmacology 37:2210-2221 doi:10.1038/npp.2012.70

O'Keefe J, Nadel L The Hippocampus as a Cognitive Map. Oxford: Clarendon Press,

O'Leary OF, Cryan JF (2014) A ventral view on antidepressant action: roles for adult hippocampal neurogenesis along the dorsoventral axis Trends Pharmacol Sci 35:675-687 doi:10.1016/j.tips.2014.09.011

O'Leary OF et al. (2014) GABAB(1) receptor subunit isoforms differentially regulate stress resilience Proc Natl Acad Sci U S A 111:15232-15237 doi:10.1073/pnas.1404090111

Olariu A, Cleaver KM, Cameron HA (2007) Decreased neurogenesis in aged rats results from loss of granule cell precursors without lengthening of the cell cycle J Comp Neurol 501:659-667 doi:10.1002/cne.21268

Overstreet Wadiche L, Bromberg DA, Bensen AL, Westbrook GL (2005) GABAergic signaling to newborn neurons in dentate gyrus J Neurophysiol 94:4528-4532 doi:10.1152/jn.00633.2005

Pace TW, Gaylord R, Topczewski F, Girotti M, Rubin B, Spencer RL (2005) Immediate-early gene induction in hippocampus and cortex as a result of novel experience is not directly related to the stressfulness of that experience Eur J Neurosci 22:1679-1690 doi:10.1111/j.1460-9568.2005.04354.x

Patricio P, Mateus-Pinheiro A, Sousa N, Pinto L (2013) Re-cycling paradigms: cell cycle regulation in adult hippocampal neurogenesis and implications for depression Mol Neurobiol 48:84-96 doi:10.1007/s12035-013-8422-x

Pinto V et al. (2015) Differential impact of chronic stress along the hippocampal dorsal-ventral axis Brain Struct Funct 220:1205-1212 doi:10.1007/s00429-014-0713-0

Rahimi O, Claiborne BJ (2007) Morphological development and maturation of granule neuron dendrites in the rat dentate gyrus Prog Brain Res 163:167-181 doi:10.1016/S0079-6123(07)63010-6

Rajkowska G, Miguel-Hidalgo JJ (2007) Gliogenesis and glial pathology in depression CNS Neurol Disord Drug Targets 6:219-233

Ramirez-Amaya V, Marrone DF, Gage FH, Worley PF, Barnes CA (2006) Integration of new neurons into functional neural networks J Neurosci 26:12237-12241 doi:10.1523/JNEUROSCI.2195-06.2006

Ramirez-Amaya V, Vazdarjanova A, Mikhael D, Rosi S, Worley PF, Barnes CA (2005) Spatial exploration-induced Arc mRNA and protein expression: evidence for selective, network-specific reactivation J Neurosci 25:1761-1768 doi:10.1523/JNEUROSCI.4342-04.2005

Ruediger S, Spirig D, Donato F, Caroni P (2012) Goal-oriented searching mediated by ventral hippocampus early in trial-and-error learning Nat Neurosci 15:1563-1571 doi:10.1038/nn.3224

Satvat E, Gheidi A, Voll S, Odintsova IV, Marrone DF (2012) Location is everything: neurons born during fluoxetine treatment accumulate in regions that do not support spatial learning Neuropharmacology 62:1627-1633 doi:10.1016/j.neuropharm.2011.11.025

Scharfman HE, Sollas AL, Smith KL, Jackson MB, Goodman JH (2002) Structural and functional asymmetry in the normal and epileptic rat dentate gyrus J Comp Neurol 454:424-439 doi:10.1002/cne.10449

Schmidt B, Marrone DF, Markus EJ (2012) Disambiguating the similar: the dentate gyrus and pattern separation Behavioural brain research 226:56-65 doi:10.1016/j.bbr.2011.08.039

Schousboe A, Waagepetersen HS (2006) Glial modulation of GABAergic and glutamat ergic neurotransmission Curr Top Med Chem 6:929-934

Seri B, Garcia-Verdugo JM, McEwen BS, Alvarez-Buylla A (2001) Astrocytes give rise to new neurons in the adult mammalian hippocampus J Neurosci 21:7153-7160

Shors TJ, Miesegaes G, Beylin A, Zhao M, Rydel T, Gould E (2001) Neurogenesis in the adult is involved in the formation of trace memories Nature 410:372-376 doi:10.1038/35066584

35066584 [pii]

Silva R, Lu J, Wu Y, Martins L, Almeida OF, Sousa N (2006) Mapping cellular gains and losses in the postnatal dentate gyrus: implications for psychiatric disorders Exp Neurol 200:321-331 doi:10.1016/j.expneurol.2006.02.119

Smith MA, Makino S, Kvetnansky R, Post RM (1995) Stress and glucocorticoids affect the expression of brain-derived neurotrophic factor and neurotrophin-3 mRNAs in the hippocampus J Neurosci 15:1768-1777

Snyder JS et al. (2009a) Adult-born hippocampal neurons are more numerous, faster maturing, and more involved in behavior in rats than in mice J Neurosci 29:14484-14495 doi:10.1523/JNEUROSCI.1768-09.2009

Snyder JS, Radik R, Wojtowicz JM, Cameron HA (2009b) Anatomical gradients of adult neurogenesis and activity: young neurons in the ventral dentate gyrus are activated by water maze training Hippocampus 19:360-370 doi:10.1002/hipo.20525

Snyder JS, Soumier A, Brewer M, Pickel J, Cameron HA (2011) Adult hippocampal neurogenesis buffers stress responses and depressive behaviour Nature 476:458-461 doi:nature10287 [pii]
10.1038/nature10287

Song H, Stevens CF, Gage FH (2002) Astroglia induce neurogenesis from adult neural stem cells Nature 417:39-44 doi:10.1038/417039a

Tannenholz L, Jimenez JC, Kheirbek MA (2014) Local and regional heterogeneity underlying hippocampal modulation of cognition and mood Front Behav Neurosci 8:147 doi:10.3389/fnbeh.2014.00147

Tanti A, Belzung C (2013) Neurogenesis along the septo-temporal axis of the hippocampus: are depression and the action of antidepressants region-specific? Neuroscience 252:234-252 doi:10.1016/j.neuroscience.2013.08.017

Tanti A, Rainer Q, Minier F, Surget A, Belzung C (2012) Differential environmental regulation of neurogenesis along the septo-temporal axis of the hippocampus Neuropharmacology doi:S0028-3908(12)00158-X [pii]
10.1016/j.neuropharm.2012.04.022

Tashiro A, Sandler VM, Toni N, Zhao C, Gage FH (2006) NMDA-receptor-mediated, cell-specific integration of new neurons in adult dentate gyrus Nature 442:929-933 doi:10.1038/nature05028

Toni N, Laplagne DA, Zhao C, Lombardi G, Ribak CE, Gage FH, Schinder AF (2008) Neurons born in the adult dentate gyrus form functional synapses with target cells Nat Neurosci 11:901-907 doi:10.1038/nn.2156

Toni N et al. (2007) Synapse formation on neurons born in the adult hippocampus Nat Neurosci 10:727-734 doi:10.1038/nn1908

Toyoda A, Iio W, Goto T, Koike H, Tsukahara T (2014) Differential expression of genes encoding neurotrophic factors and their receptors along the septal-temporal axis of the rat hippocampus Anim Sci J 85:986-993 doi:10.1111/asj.12268

Tsankova NM, Berton O, Renthal W, Kumar A, Neve RL, Nestler EJ (2006) Sustained hippocampal chromatin regulation in a mouse model of depression and antidepressant action Nat Neurosci 9:519-525 doi:nn1659 [pii]
10.1038/nn1659

Ueki T et al. (2003) A novel secretory factor, Neurogenesin-1, provides neurogenic environmental cues for neural stem cells in the adult hippocampus J Neurosci 23:11732-11740

VanElzakker M, Fevurly RD, Breindel T, Spencer RL (2008) Environmental novelty is associated with a selective increase in Fos expression in the output elements of the hippocampal formation and the perirhinal cortex Learn Mem 15:899-908 doi:10.1101/lm.1196508

Vinogradova OS (1995) Expression, control, and probable functional significance of the neuronal theta-rhythm Prog Neurobiol 45:523-583

Willner P (2005) Chronic mild stress (CMS) revisited: consistency and behavioural-neurobiological concordance in the effects of CMS Neuropsychobiology 52:90-110 doi:87097 [pii]
10.1159/000087097

Wu MV, Sahay A, Duman RS, Hen R (2015) Functional differentiation of adult-born neurons along the septotemporal axis of the dentate gyrus Cold Spring Harb Perspect Biol 7:a018978 doi:10.1101/cshperspect.a018978

Wyss JM, Swanson LW, Cowan WM (1979) Evidence for an input to the molecular layer and the stratum granulosum of the dentate gyrus from the supramammillary region of the hypothalamus Anat Embryol (Berl) 156:165-176

Youngblood BD, Zhou J, Smagin GN, Ryan DH, Harris RB (1997) Sleep deprivation by the "flower pot" technique and spatial reference memory Physiol Behav 61:249-256

Figure Legends

Fig. 1 Regional distribution of proliferation and newborn neural cells in the hippocampal DG in basal conditions. (a1) Experimental timeline and BrdU labelling protocol. (a2) Representative scheme of the DG subdivisions considered in the analysis. (a3) Representative coronal sections of the rat DG stained for Ki-67 (in red) and DAPI (in blue). (a4) Representative confocal image of the DG stained for NeuN (in green), BrdU (in red) and DAPI (in blue) (a5) and staining for GFAP (in green), BrdU (in red) and DAPI (in blue). Scale bars represent 300 and 50 μm, respectively. (b-c) Quantitative analysis of the regional preference for the location of proliferation cells, newly born neurons (d-e) and glial cells (f-g) in subregions of the hippocampal dorsal DG. Student's *t*-test. Data represented as mean ± SEM. * $P \leq 0.05$, ** $P \leq 0.01$, *** $P \leq 0.001$; n = 3-4 *per* group. Abbreviations: BrdU, bromodeoxyuridine; DAPI, 4',6-diamidino-2-phenylindole; NeuN, Neuronal nuclei; GFAP, Glial fibrillary acidic protein; SUPRA, suprapyramidal blade; INFRA, infrapyramidal blade, SGZ, subgranular zone; GCL, granule cell layer.

Fig. 2 Chronic stress exposure induces deficits in hippocampal function-related cognitive behaviors. (a) Schematic representation of the experimental timeline. (b) Animals exposed to uCMS presented elevated basal corticosterone levels in the blood serum, measured between 8 a.m and 9 a.m, at the end of the uCMS protocol. (c) Exposure to uCMS also decreased the levels of *Bdnf*, a neuroplasticity-related protein, in the hippocampal DG. (d,e) uCMS negatively affects long-term and object location memory assessed in the NOR test. (f-j) Exposure to uCMS produces deficits in reference memory (f) and behavioral flexibility (g), in the MWM test. (h) Schematic representation and color code for strategies in the reference task of the MWM. uCMS exposure delays the transition from non-hippocampal-dependent to hippocampal-dependent strategies (i, j). *Denotes the effect of uCMS analyzed by Student's *t*-test. Analysis of variance repeated measures was used to analyze cognitive learning task performance. Data are presented as mean ± SEM. $^{*}P \leq 0.05$, $^{**}P$

≤ 0.01, *** $P \leq 0.001$; n = 3-8 *per* group. Abbreviations: BrdU, bromodeoxyuridine; uCMS, unpredictable chronic mild stress protocol; MWM, Morris water maze; NOR, Novel object recognition; CTRL, non-stressed animals; *Bdnf*, brain-derived neurotrophic factor; AUC, Area under the curve.

Fig. 3. Chronic stress exposure affects the distribution of proliferating progenitor cells and survival across hippocampal DG subregions. (a) uCMS promoted a decrease in Ki-67$^+$ proliferating cells in all considered DG subregions. (b) Analysis of adult-born neurons, identified as NeuN$^+$BrdU$^+$ cells, revealed that exposure to uCMS leads to an overall decrease in the number of surviving adult-born neurons in the whole dorsal DG and in the suprapyramidal blade. (c) Analysis of the number of GFAP$^+$BrdU$^+$ cells, showed an overall decrease in the number of survived astroglial cells, not observed when considering their subregions. (d) Schematic representation of the DG and the considered subregions. Cell distributions across dorsal DG subregions and the impact of uCMS in the number of Ki-67$^+$ (e), NeuN$^+$BrdU$^+$ (f), and GFAP$^+$BrdU$^+$ (g) in the DG. *Denotes the effect of uCMS analyzed by Student's t-test. (a-c) Data are presented as mean ± SEM. Fold change relative to the CTRL group. * $P \leq 0.05$, ** $P \leq 0.01$, *** $P \leq 0.001$; n = 3-4 *per* group. Abbreviations: CTRL, non-stressed animals; SUPRA, suprapyramidal blade; INFRA, infrapyramidal blade, SGZ, subgranular zone; GCL, granule cell layer; BrdU, bromodeoxyuridine; NeuN, Neuronal nuclei; GFAP, Glial fibrillary acidic protein; uCMS, unpredictable chronic mild stress protocol.

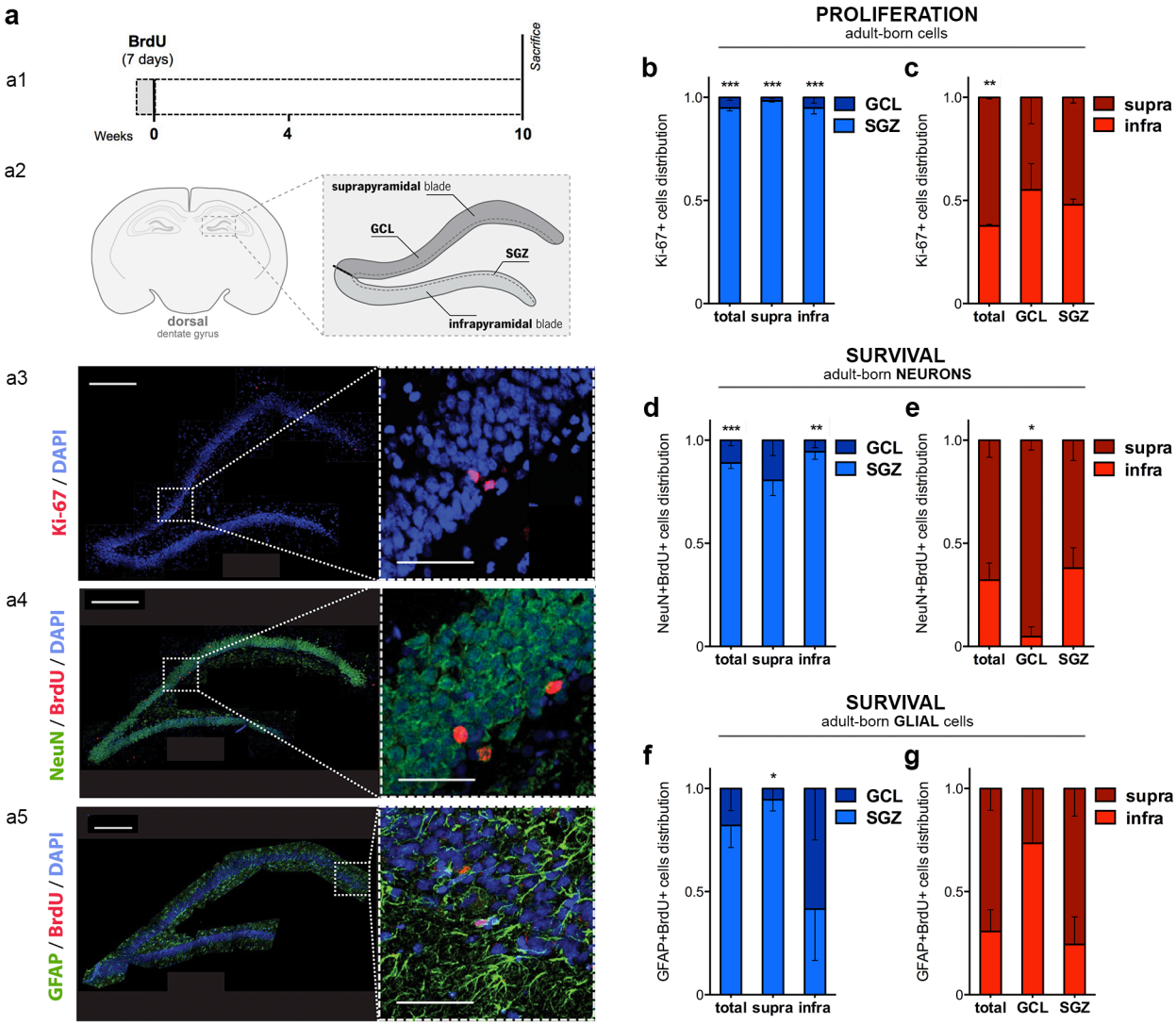
a
a1
BrdU
(7 days)
Sacrifice
Weeks 0
4
10
a2
suprapyramidal blade
GCL
SGZ
infrapyramidal blade
dorsal
dentate gyrus
a3
Ki-67 / DAPI
a4
NeuN / BrdU / DAPI
a5
GFAP / BrdU / DAPI
PROLIFERATION
adult-born cells
b
Ki-67+ cells distribution
1.0
0.5
0
***
***
***
GCL
SGZ
total supra infra
c
Ki-67+ cells distribution
**
supra
infra
total GCL SGZ
SURVIVAL
adult-born NEURONS
d
NeuN+BrdU+ cells distribution
***
**
GCL
SGZ
total supra infra
e
NeuN+BrdU+ cells distribution
*
supra
infra
total GCL SGZ
SURVIVAL
adult-born GLIAL cells
f
GFAP+BrdU+ cells distribution
*
GCL
SGZ
total supra infra
g
GFAP+BrdU+ cells distribution
supra
infra
total GCL SGZ

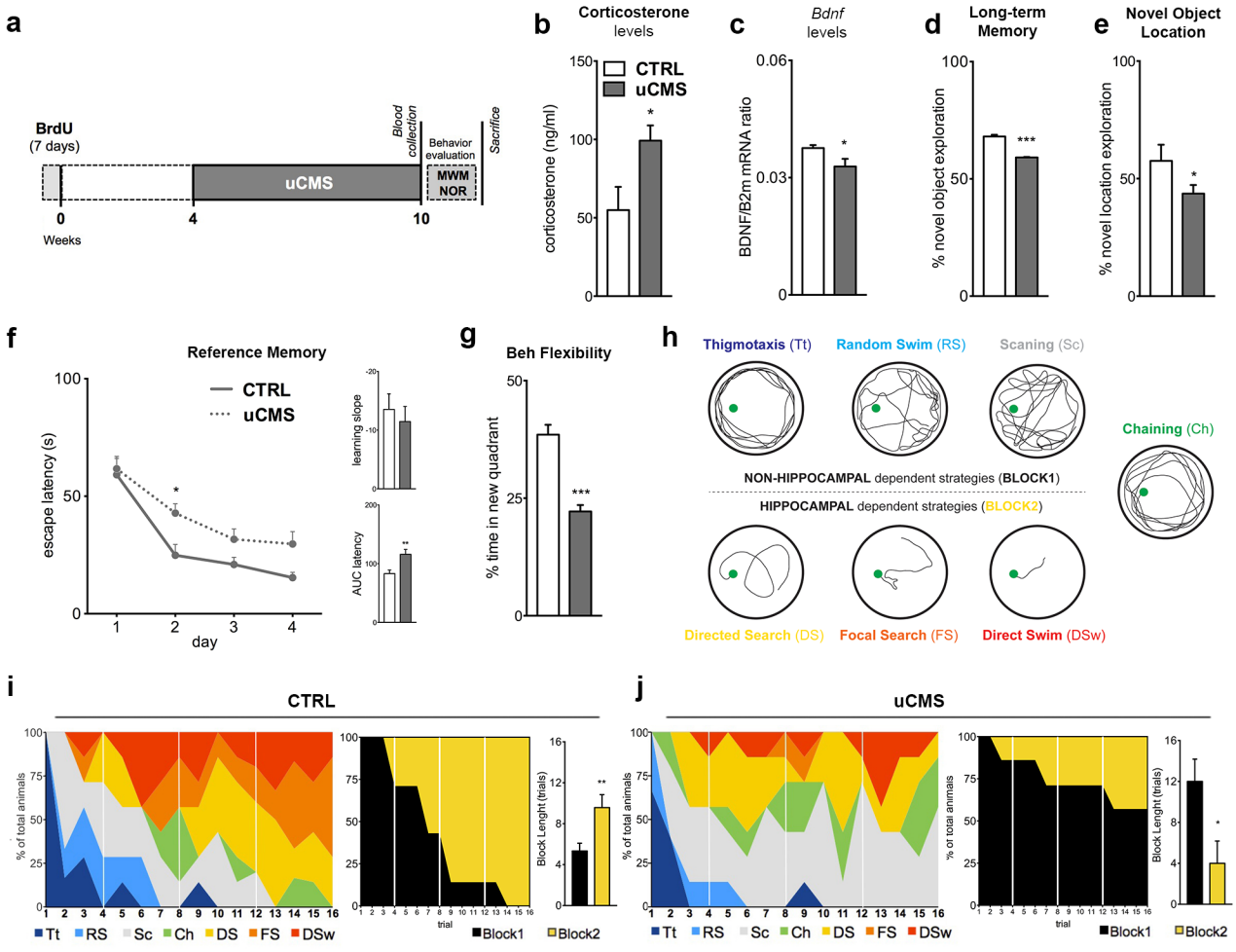
a
BrdU
(7 days)
uCMS
Blood collection
Behavior evaluation
MWM
NOR
Sacrifice
0
4
10
Weeks
b
Corticosterone levels
CTRL
uCMS
corticosterone (ng/ml)
c
Bdnf levels
BDNF/B2m mRNA ratio
d
Long-term Memory
% novel object exploration
e
Novel Object Location
% novel location exploration
f
Reference Memory
escape latency (s)
day
learning slope
AUC latency
g
Beh Flexibility
% time in new quadrant
h
Thigmotaxis (Tt)
Random Swim (RS)
Scaning (Sc)
Chaining (Ch)
NON-HIPPOCAMPAL dependent strategies (BLOCK1)
HIPPOCAMPAL dependent strategies (BLOCK2)
Directed Search (DS)
Focal Search (FS)
Direct Swim (DSw)
i
CTRL
% of total animals
Tt RS Sc Ch DS FS DSw
trial
Block Lenght (trials)
Block1
Block2
j
uCMS

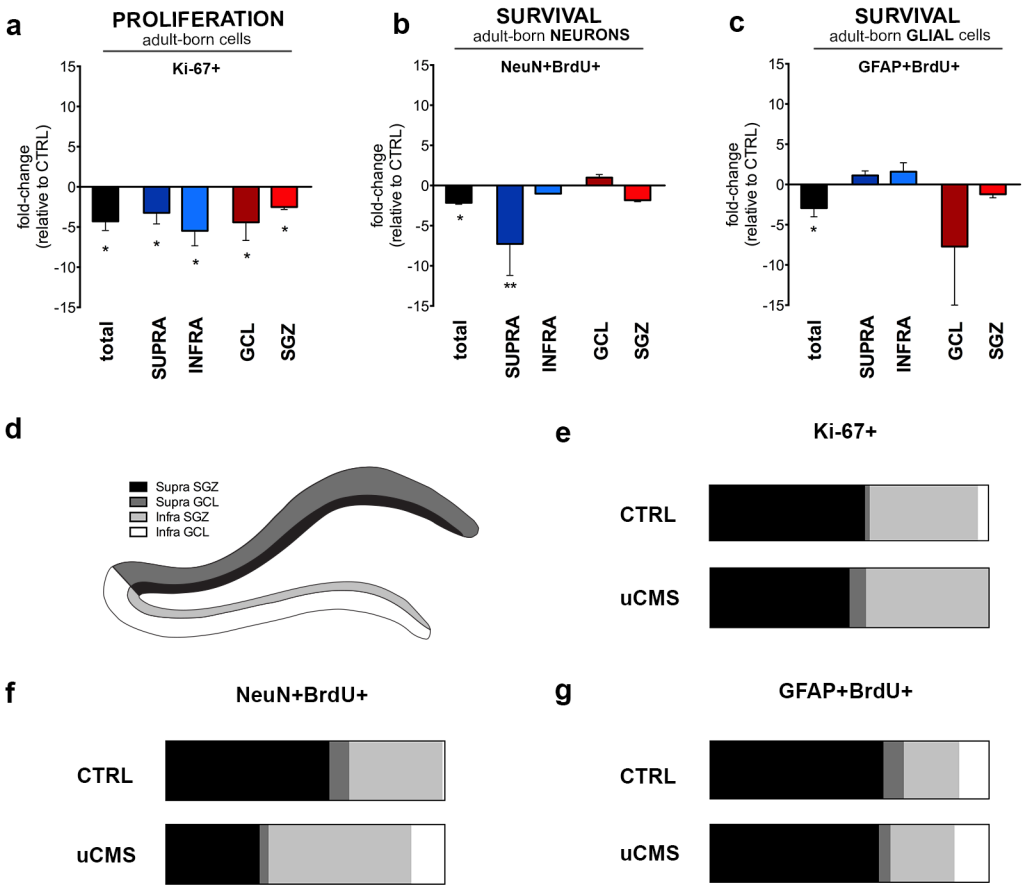
a
PROLIFERATION
adult-born cells
Ki-67+
b
SURVIVAL
adult-born NEURONS
NeuN+BrdU+
c
SURVIVAL
adult-born GLIAL cells
GFAP+BrdU+
fold-change (relative to CTRL)
15
10
5
0
-5
-10
-15
total
SUPRA
INFRA
GCL
SGZ
d
Supra SGZ
Supra GCL
Infra SGZ
Infra GCL
e
Ki-67+
CTRL
uCMS
f
NeuN+BrdU+
CTRL
uCMS
g
GFAP+BrdU+
CTRL
uCMS

Table 1. Cell densities among distinct neural populations in the different DG subregions, in both basal conditions and after chronic stress exposure. Data are presented as mean ± SEM.

Cell densities (cells/mm^2)	Ki-67$^+$			BrdU$^+$NeuN$^+$			BrdU$^+$GFAP$^+$		
	CTRL	uCMS	*P*	CTRL	uCMS	*P*	CTRL	uCMS	*P*
DG	42.61 (±11.67)	9.918 (±2.63)	0.0261*	23.75 (±6.21)	11.03 (±0.87)	0.0308*	10.74 (±2.92)	3.660 (±1.34)	0.0461*
SGZ	59.87 (±14.39)	23.93 (±2.91)	0.0353*	40.07 (±13.33)	21.79 (±2.06)	0.1507	25.78 (±10.52)	21.43 (±8.11)	0.3760
GCL	4.692 (±1.22)	1.267 (±0.65)	0.0387*	3.184 (±0.93)	3.241 (±1.29)	0.4874	2.698 (±1.42)	0.3503 (±0.35)	0.1137
Supra DG	31.27 (±8.52)	9.681 (±4.16)	0.0495*	31.09 (±1.88)	4.278 (±2.31)	0.0019**	9.330 (±4.14)	10.46 (±5.28)	0.4359
Infra DG	49.36 (±17.67)	9.036 (±3.08)	0.0439*	17.31 (±2.37)	17.27 (±0.79)	0.4918	6.853 (±2.37)	10.96 (±7.62)	0.3128

Table 2. Distribution of neural populations in the distinct DG subregions, in both basal conditions and after chronic stress exposure. Data are presented as mean ± SEM.

Cell distribution (%)	Ki-67$^+$				BrdU$^+$NeuN$^+$				BrdU$^+$GFAP$^+$			
	CTRL		uCMS		CTRL		uCMS		CTRL		uCMS	
SGZ	94.87	(±1.4)	94.03	(±3.4)	88.95	(±2.7)	86.03	(±5.2)	82.13	(±10.7)	97.68	(±2.3)
GCL	5.13		5.97		11.05		13.97		17.87		2.32	
Infra DG	37.66	(±8.0)	42.38	(±13.2)	32.15	(±8.3)	73.65	(±10.0)	30.68	(±10.6)	35.89	(±22.2)
Supra DG	62.34		57.62		67.85		26.35		69.32		64.11	
Infra SGZ	47.89	(±2.7)	50	(±9.6)	37.99	(±9.8)	70.60	(±11.4)	24.41	(±13.4)	10.87	(±10.9)
Supra SGZ	52.11		50		62.01		29.40		75.59		89.13	
Infra GCL	55.09	(±12.7)	0	(±0)	4.75	(±4.7)	77.78	(±11.1)	73.43	(±26.6)	85.85	(±14.1)
Supra GCL	44.91		100		95.25		22.22		36.57		14.15	

Table 3. Total regional distribution of neural populations in DG subregions, in basal conditions and after chronic stress exposure. Data are presented as mean ± SEM.

Cell distribution (%)	Ki-67$^+$		BrdU$^+$NeuN$^+$		BrdU$^+$GFAP$^+$	
	CTRL	uCMS	CTRL	uCMS	CTRL	uCMS
Infra SGZ	38.7 (±6.7)	44.1 (±12.1)	33.4 (±9.8)	51.2 (±2.3)	19.0 (±10.0)	22.9 (±19.4)
Supra SGZ	55.8 (±4.6)	50.0 (±9.6)	58.6 (±7.6)	33.6 (±8.2)	62.1 (±6.4)	60.5 (±23.1)
Infra GCL	3.8 (±2.4)	0 (±0)	0.9 (±0.9)	12.0 (±6.1)	10.7 (±5.4)	12.4 (±9.9)
Supra GCL	1.7 (±0.7)	5.9 (±3.0)	7.1 (±1.8)	3.2 (±2.1)	7.3 (±7.3)	4.1 (±4.1)